



**HAL**  
open science

## Preparation of iron cobaltite thin films by RF magnetron sputtering

Hoa Le Trong, Thi Mai Anh Bui, Lionel Presmanes, Antoine Barnabé,  
Isabelle Pasquet, Corine Bonningue, Philippe Tailhades

► **To cite this version:**

Hoa Le Trong, Thi Mai Anh Bui, Lionel Presmanes, Antoine Barnabé, Isabelle Pasquet, et al.. Preparation of iron cobaltite thin films by RF magnetron sputtering. *Thin Solid Films*, 2015, vol. 589, pp. 292-297. 10.1016/j.tsf.2015.05.041 . hal-01168678

**HAL Id: hal-01168678**

**<https://hal.science/hal-01168678>**

Submitted on 26 Jun 2015

**HAL** is a multi-disciplinary open access archive for the deposit and dissemination of scientific research documents, whether they are published or not. The documents may come from teaching and research institutions in France or abroad, or from public or private research centers.

L'archive ouverte pluridisciplinaire **HAL**, est destinée au dépôt et à la diffusion de documents scientifiques de niveau recherche, publiés ou non, émanant des établissements d'enseignement et de recherche français ou étrangers, des laboratoires publics ou privés.



## Open Archive Toulouse Archive Ouverte (OATAO)

OATAO is an open access repository that collects the work of Toulouse researchers and makes it freely available over the web where possible.

This is an author-deposited version published in: <http://oatao.univ-toulouse.fr/>  
Eprints ID: 13980

**Identification number:** DOI: 10.1016/j.tsf.2015.05.041  
**Official URL:** <http://dx.doi.org/10.1016/j.tsf.2015.05.041>

**To cite this version:**

Le Trong, Hoa and Bui, Thi Mai Anh and Presmanes, Lionel and Barnabé, Antoine and Pasquet, Isabelle and Bonningue, Corine and Tailhades, Philippe  
*Preparation of iron cobaltite thin films by RF magnetron sputtering.* (2015)  
Thin Solid Films, vol. 589. pp. 292-297. ISSN 0040-6090

Any correspondence concerning this service should be sent to the repository administrator:  
[staff-oatao@inp-toulouse.fr](mailto:staff-oatao@inp-toulouse.fr)

# Preparation of iron cobaltite thin films by RF magnetron sputtering

H. Le Trong<sup>a,b,c</sup>, T.M.A. Bui<sup>a,b,d</sup>, L. Presmanes<sup>a,b,\*</sup>, A. Barnabé<sup>a,b</sup>, I. Pasquet<sup>a,b</sup>, C. Bonningue<sup>a,b</sup>, Ph. Tailhades<sup>a,b</sup>

<sup>a</sup> Université de Toulouse, UPS, INPT, Institut Carnot CIRIMAT, 118, Route de Narbonne, F-31062 Toulouse cedex 9, France

<sup>b</sup> CNRS, Institut Carnot Cirimat, F-31062 Toulouse, France

<sup>c</sup> Ho Chi Minh City University of Science, Vietnam National University Ho Chi Minh City, 227 Nguyen Van Cu Q.5, 750000 Ho Chi Minh City, Viet Nam

<sup>d</sup> University of Transport and Communications, Lang Thuong, Dong Da, Hanoi, Viet Nam

## A B S T R A C T

Iron cobaltite thin films with spinel structure have been elaborated by radio-frequency (RF) magnetron sputtering from a  $\text{Co}_{1.75}\text{Fe}_{1.25}\text{O}_4$  target. Influence of argon pressure on structure, microstructure and physical properties of films has been examined. Iron–cobalt oxide thin films essentially consist of one spinel phase when deposited at low pressure (0.5 and 1.0 Pa). At high pressure (2.0 Pa), the global stoichiometry of the film is changed which results in the precipitation of a mixed monoxide of cobalt and iron beside the spinel phase. This in-situ reduction due to an oxygen loss occurring mainly at high deposition pressure has been revealed by X-ray diffraction and Raman spectroscopy. Microstructural evolution of thin film with argon pressure has been shown by microscopic observations (AFM and SEM). The evolution of magnetic and electrical properties, versus argon pressure, has been also studied by SQUID and 4 probe measurements.

## Keywords:

Thin film  
Sputtering  
Cobaltite  
Spinel oxide  
Magnetic coupling  
Exchange field  
Monoxide  
In-situ reduction

## 1. Introduction

Transition-metal oxides with spinel structure have been intensively investigated over decades for potential technological applications due to their variety of interesting physical and chemical properties. Spinel oxides are described by the general formula  $A[\text{B}_2]\text{O}_4$  with A and B representing tetrahedral (Td) and octahedral (Oh) sites, respectively. The divalent cations occupy Td sites and the trivalent cations occupy Oh sites in normal spinels [1]. But for disordered spinels or inverse spinels, tetrahedral sites can be occupied partially or totally by the trivalent cations [2–5]. Such structure tends to exhibit varying physical properties depending on nature of transition-metal cations and their distribution between two crystalline sites [6,7].

Iron cobaltites exhibit excellent chemical stability and high corrosion resistance. These semiconductors with relatively high activation energy and negative temperature coefficient are interesting as sensitive elements in uncooled bolometers [8]. Attractive magnetic properties (large coercivity, magneto-crystalline anisotropy and magnetostriction [9]) make cobalt–iron spinel oxides, especially in thin films form, potential candidates for magnetic devices. In addition, spinel cobaltites are

also of interest for various applications due for example to their thermoelectric [10,11], multiferroic [12,13] or catalytic [14,15] properties.

Iron cobaltites for which the composition lies between  $\text{CoFe}_2\text{O}_4$  and  $\text{Co}_3\text{O}_4$  are located in a miscibility gap of the Co–Fe–O phase diagram that leads to the precipitation of a mixture of iron-rich and cobalt-rich spinel phases at low temperature [16,17]. When its composition is in between  $\text{Co}_{1.10}\text{Fe}_{1.85}\text{O}_4$  and  $\text{Co}_{2.75}\text{Fe}_{0.25}\text{O}_4$ , a pure spinel can be easily obtained by annealing this oxide at 900 °C and quenching down to room temperature to avoid the phase separation [18,19]. It is itself a first challenge to deposit a pure and metastable spinel oxide thin film in the miscibility gap area without any thermal treatment requirement. From this pure spinel pristine phase obtained in the miscibility gap of the phase diagram, it is then possible to obtain self-organized materials by spinodal decomposition at low temperature [20]. Such a spontaneous transformation has a great interest because it can promote a regular alternation, at nanometric scale, of magnetically ordered phases made of iron-rich and cobalt-rich spinel oxides [21–24]. The study of spinodal decomposition of magnetically ordered phases could lead to original properties. For example giant magnetoresistance was thus observed in ferromagnetic alloys obtained from spinodal decomposition [25,26]. Other collective properties could be generated in these potential self-organized metamaterials to get for instance magnonic crystals [27,28].

In this study, spinel thin films were prepared by radio-frequency magnetron sputtering from a  $\text{Co}_{1.75}\text{Fe}_{1.25}\text{O}_4$  ceramic target. The composition was chosen to be close to the centerline of the miscibility gap observed in the  $\text{CoFe}_2\text{O}_4$ – $\text{Co}_3\text{O}_4$  phase diagram. We particularly studied

\* Corresponding author at: Université de Toulouse, UPS, INPT, Institut Carnot CIRIMAT, 118, route de Narbonne, F-31062 Toulouse cedex 9, France. Tel.: +33 561558103; fax: +33 561556163.

E-mail address: presmane@chimie.ups-tlse.fr (L. Presmanes).

the influence of deposition pressure on structure, microstructure and physical properties of films in order to get pure metastable phase at room temperature.

## 2. Experimental

### 2.1. Films preparation

Thin films were deposited by magnetron radio-frequency (RF) magnetron sputtering using a  $\text{Co}_{1.75}\text{Fe}_{1.25}\text{O}_4$  ceramic target, which has been elaborated from mechanical mixture of  $\text{Co}_3\text{O}_4$  and  $\text{Fe}_3\text{O}_4$  commercial powders. The powder mixture was pressed in a die and the green disc (20 cm in diameter and 5 mm thick) was slowly heated to eliminate the organic binder and then sintered at 900 °C for 12 h under air atmosphere. After a second heat treatment carried out at 950 °C for 4 h under air, the target density was close to 60% and the final diameter was 19 cm. The composition of the target was checked by plasma emission spectroscopy carried out in a small representative pellet prepared at the same time. The analysis of the chemical composition of the films by electron probe micro-analysis (using a Cameca SX 50 apparatus) confirmed the conservation into the film of the cationic composition of the target: all the samples showed a constant cationic ratio Co/Fe closed to 1.4 regardless of the deposition pressure.

The sputtering apparatus is an ALCATEL CIT model SCR650 equipped with a radio-frequency-generator (13.56 MHz) device as well as a pumping system (a mechanical pump coupled with a turbo molecular pump). Both target and substrate were continuously water cooled. The RF power was fixed at 1.3 W/cm<sup>2</sup> and the pressure inside the deposition chamber was lower than  $5.10^{-5}$  Pa before deposition. Pre-sputtering by argon plasma was performed during 15 min to clean the surface of the target of any impurities prior to the film deposition. Pre-cleaned 1 mm thick microscopy slides were used as substrates. In this work, P0.5D6, P1.0D6 and P2.0D6 designations refer to samples produced with an argon pressure of 0.5, 1.0 and 2.0 Pa respectively, and a target-to-substrate distance fixed at 6 cm.

For all the films, the deposition rates (Table 1) were calculated from the deposition times and thickness measurements using a DEKTAK 3030ST mechanical profilometer. Film thicknesses were set at 300 nm for all the characterizations. For magnetic measurements, the deposition was made on both faces of thinner glass substrate (0.1 mm).

### 2.2. Characterizations

Structural characterizations of films were performed at room temperature by grazing angle X-ray diffraction ( $\alpha = 1$  deg.) on a Siemens D 5000 diffractometer equipped with a Brucker Sol-X detector. The X-ray wavelength was that of the copper  $K_{\alpha}$  ray ( $K_{\alpha 1} = 0.15405$  nm and  $K_{\alpha 2} = 0.15443$  nm).

Raman spectra were collected under ambient conditions using a LabRAM HR 800 Jobin Yvon spectrometer with a laser excitation wavelength of 632.8 nm. Spectra acquisition was carried out for 400 s using  $\times 100$  objective lens and 600 g/mm grating. During the measurement, the resulting laser power at the surface of the sample was adjusted to 0.7 mW to avoid the transformation of the ferrite thin film (especially to avoid spinodal decomposition). Examination of multiple spots showed that the samples were homogeneous.

**Table 1**  
Deposition parameters.

Target diameter (cm)	19
Target-to-substrate distance (cm)	6
RF power density (W/cm <sup>2</sup> )	1.3
Sputtering gas	Ar
Background pressure (Pa)	$5.10^{-5}$
Working pressure (Pa)	0.5–1.0–2.0
Film thickness (nm)	300

To study the microstructure of the films, Atomic Force Microscopy (AFM) Veeco Dimension 3000 equipped with a super sharp TESP-SS Nanoworld@tip (nominal resonance frequency 320 kHz, nominal radius curvature 2 nm) was used. The microstructure of the samples was also investigated by scanning electron microscopy (SEM) with a JEOL JSM 6700F apparatus with a field emission gun.

Magnetic measurements were done at 300 K, 150 K and 5 K after a field cool with a superconducting quantum interference device (SQUID) magnetometer MPMS Quantum Design 5.5. The maximal applied field for the measurements was 70 kOe. The magnetizations of the samples were corrected for substrate contribution.

Films resistivity was determined by a four point measuring device composed of a source measure unit KEITHLEY 237, a high temperature four point probe QUAD PRO Resistivity System and a temperature controller SIGNATONE model S-1060R. This type of generator can measure a maximum resistance of  $10^{10}$   $\Omega$ .

## 3. Results and discussion

### 3.1. Structural characterizations

Fig. 1 shows X-ray diffraction patterns of iron cobaltite thin films deposited at different argon pressures. The patterns of all the films deposited at 0.5 and 1.0 Pa show the diffraction lines corresponding to cubic spinel structure without any secondary or impurity phases. However, film deposited at 2.0 Pa consists of two phases: a spinel phase and a monoxide phase with wüstite structure. Both CoO and FeO have wüstite structure with two lattice parameters very close each other:  $a = 4.2612$  Å for CoO (PDF #48-1719) and  $a = 4.3260$  Å for FeO (PDF #89-0687). Phase diagram of  $\text{Fe}_3\text{O}_4$ – $\text{Co}_3\text{O}_4$  system shows that spinel phase and monoxide phase can co-exist at thermodynamical equilibrium for temperatures higher than 950 °C [16,17]. Thus it is proposed that the monoxide phase formed in thin film deposited at 2.0 Pa is a Co-Fe mix monoxide ( $\text{Co}_y\text{Fe}_{1-y}\text{O}$ ). The formation of a composite monoxide/spinel oxide is in good agreement with the results reported by B. Mauvernay et al. [29] in which the  $\text{FeO}/\text{Fe}_3\text{O}_4$  nanocomposite films were deposited from a magnetite target at high argon pressure.

Formation of a monoxide phase in thin films deposited at high argon pressure can be explained by sputtering principle [30,31]. During the sputtering at high argon pressure, target is submitted to intense bombardment by high energy  $\text{Ar}^+$ , which leads to a local overheating of target surface. Such target, in a low oxygen partial pressure, tends to exhibit a reduction on its extreme surface [32]. In addition, a high

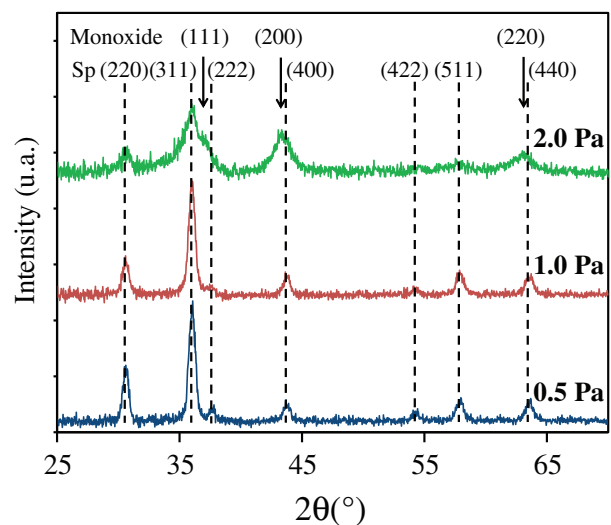


**Fig. 1.** X-ray diffraction patterns of thin films deposited at different argon pressures (sp = spinel).

number of collisions between particles ejected in the plasma induces a great ‘thermalization’ of oxygen atoms which are lighter and much more captured by pumping system than metal atoms. Accordingly, sputtering at high argon pressure shows an impoverishment of the oxygen content in the deposited films [33].

Difference in phase component for obtained films was also investigated by Raman spectroscopy and the resulting spectra are depicted in Fig. 2. Films deposited at 0.5 and 1.0 Pa have similar spectra, which are exactly the same as the spectrum of a pure  $\text{Co}_{1.7}\text{Fe}_{1.3}\text{O}_4$  ceramic that we have already published elsewhere [33]. The spectra exhibit five Raman-active modes of spinel structure [34,35] in this spectral range:  $3F_{2g}$  ( $185$ ,  $325$  and  $640\text{ cm}^{-1}$ ),  $E_g$  ( $490\text{ cm}^{-1}$ ) and  $A_{1g}$  ( $695\text{ cm}^{-1}$ ). The position of these peaks is in good accordance with the reported value for cobalt–iron spinel oxides [36,37]. Two peaks at high Raman shifts  $F_{2g}(3)$  ( $640\text{ cm}^{-1}$ ) and  $A_{1g}$  ( $695\text{ cm}^{-1}$ ) are assigned to the vibrations of cations and oxygen ions in Td sites [36,38–40]. Three peaks at low Raman shifts  $F_{2g}(1)$  ( $185\text{ cm}^{-1}$ )  $F_{2g}(2)$  ( $325\text{ cm}^{-1}$ )  $E_g$  ( $490\text{ cm}^{-1}$ ) are attributed to the vibrations of cations and oxygen ions in Oh sites [38–40].

However, Raman spectra of films deposited at 2.0 Pa shows only two peaks ( $550$  and  $630\text{ cm}^{-1}$ ), one of them (peak at  $630\text{ cm}^{-1}$ ) is attributed to peak  $F_{2g}(3)$  of spinel phase. The peak at  $550\text{ cm}^{-1}$  possibly results from the formation of monoxide phase in this film. For spectral range from  $450$  to  $600\text{ cm}^{-1}$ , Raman spectrum of FeO presents one peak at  $595\text{ cm}^{-1}$  [41] and the one of CoO exhibits one peak at  $455\text{ cm}^{-1}$ . Therefore, monoxide phase formed in films deposited at 2.0 Pa, is coherent with the formation of a mix monoxide of cobalt and iron. This is in good accordance with above-mentioned X-ray diffraction analysis.

### 3.2. Microstructural characterizations

Atomic force microscopy (AFM) and scanning electron microscopy (SEM) analyses show a homogenous microstructure for both films deposited at 0.5 and 2.0 Pa. The film deposited at 0.5 Pa is made of small grains of about 30 to 40 nm in diameter (Fig. 3a). The Ra roughness of the films, determined by AFM, is close to 1.9 nm. SEM cross-section view of this film (Fig. 3b) shows a structure characteristic of films deposited by sputtering with well-crystallized columns. Films deposited at 2.0 Pa are formed of smaller and more circular grains (15 to 30 nm) (Fig. 3c) and they have a smaller Ra roughness (0.9 nm). These films exhibit narrower columns, which tend to divide into fragments (Fig. 3d). The change in microstructure of films deposited at 2.0 Pa, may be due

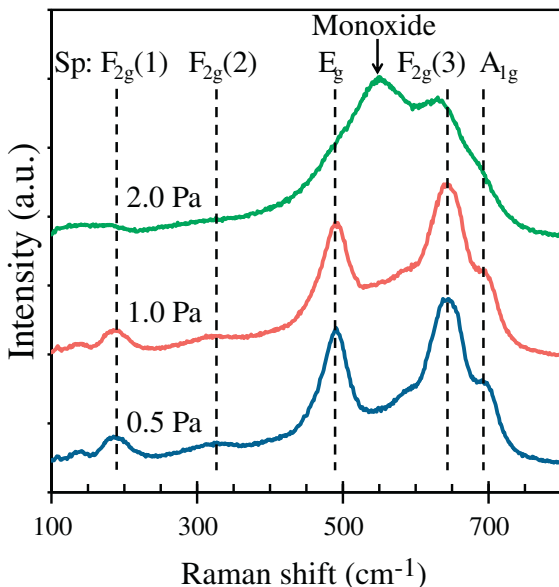


Fig. 2. Raman spectra of thin films deposited at different argon pressure (sp = spinel).

to the fact that they contain small alternate crystalline domains of spinel phase and monoxide phase.

### 3.3. Magnetic properties

Magnetic properties were registered at 300 K under a maximal magnetic field of 70 kOe parallel to the film plane (in-plane measurement). Fig. 4 presents in-plane hysteresis loops registered at 300 K for films deposited at different argon pressures.

The saturation magnetization ( $M_s$ ) was evaluated using the last three points of the magnetization curve by plotting the magnetization as a function of the inverse of the applied magnetic field  $M = f(1/H)$ . The  $M_s$  value was obtained by extrapolation to infinite field ( $1/H = 0$ ). The saturation magnetization and the coercive force of the samples are given in Table 2.

Saturation magnetization of the sample P0.5D6 is  $118\text{ emu/cm}^3$  at 300 K. In comparison, magnetization measured on cobaltite powder with the same composition is  $39.3\text{ emu/g}$  [24] which corresponds to a value of volume magnetization closed to  $216\text{ emu/cm}^3$  by taking a density of  $5.5\text{ g/cm}^3$  for the iron–cobalt spinel oxide. This lower value of the magnetization in the case of thin film cobaltite cannot be explained by the presence of porosity. Indeed, it was shown that ferrite thin films deposited by RF sputtering from a ceramic target, at 0.5 Pa, are dense due to low shadowing effects during the film growth [42,43]. Most of the articles related to magnetic properties of oxide thin films obtained by sputtering further show that the samples obtained have much lower saturation magnetization than those measured on bulk materials [29,44,45]. This phenomenon is generally ascribed to the presence of defects [46].

When the deposition pressure is increased, the saturation magnetization drops considerably. F. Oudrhiri-Hassani [42] showed that the increase in porosity is only 15% when the pressure goes from 0.5 to 2 Pa, for ferrite thin films deposited by RF sputtering. This small increase in porosity cannot explain the dramatic decrease of the magnetization. The latter is mainly due to the disappearance of the ferromagnetic [47] spinel phase, which is gradually replaced by anti-ferromagnetic [48,49] monoxide phase when the deposition pressure increases. The sample P2.0D6, which has no coercive field and a very low saturation magnetization, seems to be a nearly pure monoxide. Changes in magnetic properties appear to be much more sensitive than X-Ray diffraction and Raman spectroscopy. In particular, the sample P1.0D6 has a lower magnetization than that measured for the sample P0.5D6 deposited at lower pressure while XRD and Raman spectra are similar for both samples. Thanks to magnetic measurements, it is therefore clear that monoxide concentration is higher in sample P1.0D6 even though it was impossible to detect its presence by another method.

Then, the samples were cooled down under the maximal field (70 kOe) until 150 K to register again hysteresis loops at this temperature. The cooling under magnetic field creates a coupling effect between the antiferromagnetic and ferrimagnetic phases that are at nanometric scale in these thin films. This is confirmed by the appearance of a magnetic coupling represented by exchange field value (Table 3). This coupling results from the magnetic interactions with the nanometric spinel (ferrimagnetic) and monoxide phase (anti-ferromagnetic) when films are cooled under magnetic field from room temperature down to temperatures lower than Néel temperature of the mix  $(\text{Co}_y\text{Fe}_{1-y})\text{O}$  monoxide phase. This temperature, which was not precisely determined, is estimated in between 290 and 185 K, which are the Neel temperatures for the two end-members of the  $(\text{Co}_y\text{Fe}_{1-y})\text{O}$  solid solution, CoO and FeO respectively [48–50]. The increase of exchange field absolute value when argon pressure increases, confirms that the higher argon pressure is, the more monoxide phase forms.

Moreover, the highlight of an exchange field for the film deposited at 0.5 Pa indicates the precipitation of a very small quantity of monoxide, which cannot be avoided even at low pressure. This monoxide phase is nanocrystallized and then cannot be observed in X-Ray diffraction

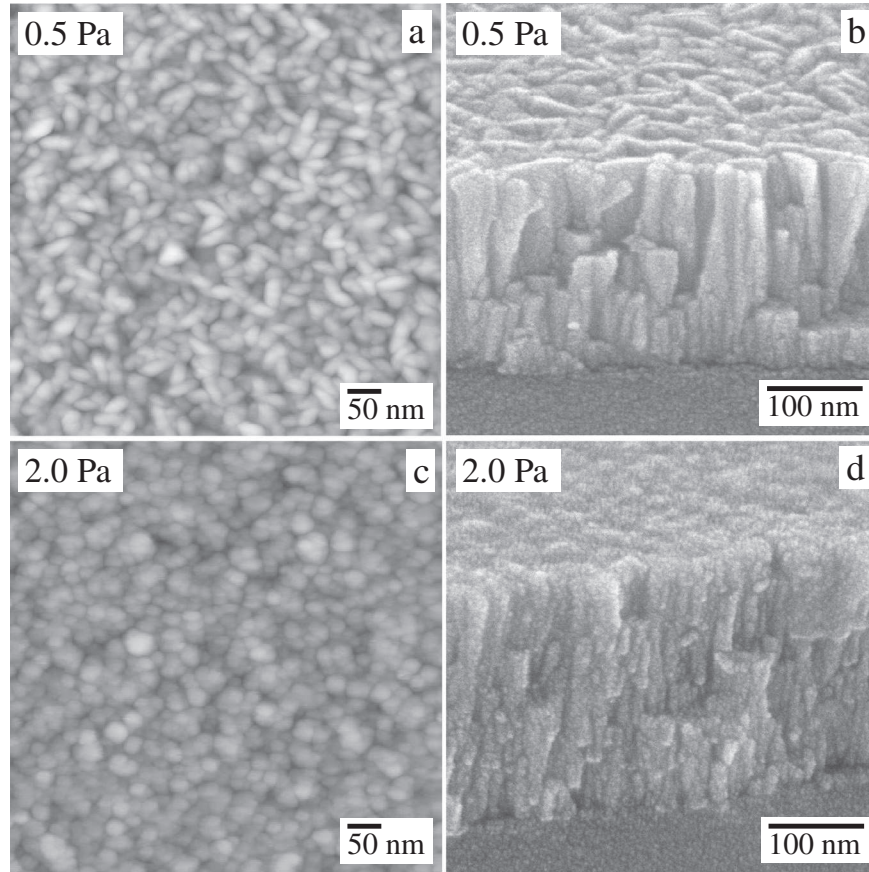


Fig. 3. AFM (a, c) and SEM (b, d) micrographs of thin films deposited at 0.5 Pa and 2.0 Pa respectively.

patterns. This phenomenon is confirmed by the measurement of an exchange field of 1295 Oe at 5 K (Fig. 5). Furthermore, the coercive force is very high at this temperature, close to 32 kOe.

### 3.4. Electrical properties

Electrical properties of all the films were also investigated. The activation energy calculated in between 20 and 70 °C varies from 0.4 to 0.5 eV. This is in good accordance with studies on electron hopping conduction between  $\text{Co}^{2+}$  and  $\text{Co}^{3+}$  cations in Oh sites of cobalt-iron oxides [51–53]. Film resistivity increases when argon pressure increases,

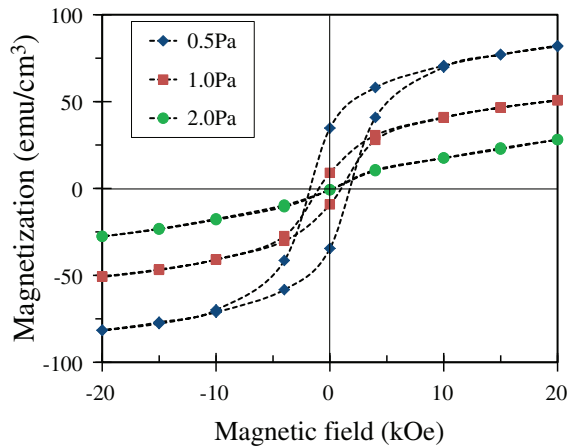


Fig. 4. In-plane hysteresis loops registered at 300 K under a maximum magnetic field of 70 kOe for thin films deposited at different argon pressures (zoomed to  $\pm 20$  kOe scale).

especially from 1.0 to 2.0 Pa (Fig. 6). The increase in resistivity is probably due to the formation of the monoxide phase, which reduces the number of  $\text{Co}^{2+}/\text{Co}^{3+}$  couples in films deposited at high argon pressure. In the same way, B. Mauvernay et al. [29] showed that resistivity of  $\text{Fe}_3\text{O}_4$ -FeO composite thin films deposited by sputtering, increases when the monoxide phase quantity grows, leading to the reduction of  $\text{Fe}^{2+}/\text{Fe}^{3+}$  couple numbers in the spinel oxide in this case. In addition, the increase of thin films inter-granular porosity versus deposition pressure can also contribute to the increase in resistivity versus argon pressure. Indeed, F. Oudrhiri-Hassani et al. [42] and S. Capdeville et al. [43] have shown a strong increase of the inter-granular porosity for the highest deposition pressures. The surface enhancement factor (surface area divided by projected area) was about 20 to 55 times higher for the films deposited at 2.0 Pa than for those made at 0.5 Pa. Electrical measurements revealed a strong dependence of the resistivity versus the inter-grain porosity. Impedance spectroscopy confirmed that the overall resistivity of the films was mainly due to the low conduction of the inter-grain area. In our case, the increase in resistivity with the deposition pressure, is then attributed to both a decrease in  $\text{Co}^{2+}/\text{Co}^{3+}$  couple number and an increase in inter-granular porosity.

Table 2

Saturation magnetization and coercive field measured at 300 K for films deposited at different argon pressures.

Argon pressure (Pa)	Saturation magnetization ( $\text{emu}/\text{cm}^3$ )	Coercive field (Oe)
0.5	118	2000
1.0	89	740
2.0	19	0

**Table 3**  
Exchange field measured at 150 K for films deposited at different argon pressures.

Argon pressure (Pa)	Exchange field (Oe) at 150 K
0.5	-95
1.0	-130
2.0	-750

#### 4. Conclusion

Iron cobaltite thin films have been elaborated by RF magnetron sputtering. Structure and microstructure of thin films depend strongly on argon pressure. Deposition at high argon pressure promotes the formation of monoxide phase that grows in competition with the spinel phase due to oxygen loss. The columns become fragmented with small alternate crystalline domains of spinel phase and monoxide phase. The increase in argon pressure also leads to the lowering of both saturation magnetization, coercive field and electrical conductivity and a bias field is observed when the magnetic hysteresis curve of the sample is measured after field cooling from room temperature to 150 K or below. This bias field is related to a coupling effect at low temperature between the ferrimagnetic spinel oxide and the antiferromagnetic monoxide.

Even if the films deposited at 0.5 and 1.0 Pa seemed to be made up of a pure spinel phase according to X-ray diffraction and Raman spectroscopy analysis, the formation of the monoxide phase in a very small quantity has been highlighted in both films deposited at 0.5 and 1.0 Pa thanks to the extreme sensitivity of magnetic coupling effects which can reveal antiferromagnetic nanoscale impurities, coupled to a ferrimagnetic phase. Our work confirms that magnetic measurements are particularly suitable for determining the presence of antiferromagnetic impurities in a ferrimagnetic matrix.

More globally, sputtering process is not only a simple physical way to prepare thin films but it allows as well the preparation of out-of-equilibrium oxides or compounds at low temperature. In our case, for example, the deposition of an iron cobaltite led, at room temperature, to a film containing a metastable  $\text{Co}_{1.75}\text{Fe}_{1.25}\text{O}_4$  phase instead of stable mixture of  $\text{Co}_{1.10}\text{Fe}_{1.85}\text{O}_4$  and  $\text{Co}_{2.75}\text{Fe}_{0.25}\text{O}_4$ , as it could be expected from the phase diagram. Moreover, we also showed that sputtering deposition acts like a chemical reactor in which the intensity of reduction reactions can easily be managed by fine-tuning the deposition parameters. That leads to the formation of reduced thin films by impoverishment of the oxygen content in the growing layer. Such a film can be composed of a pure and metastable reduced phase, or it can contain a mixture of stoichiometric and reduced phases or even only reduced phases, depending on the parameter settings during this easy-to-

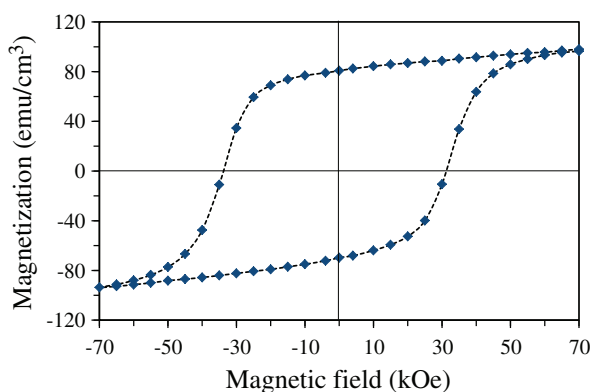


**Fig. 5.** In-plane hysteresis loop registered at 5 K under a maximum magnetic field of 70 kOe for thin films deposited at 0.5 Pa (field cooled).

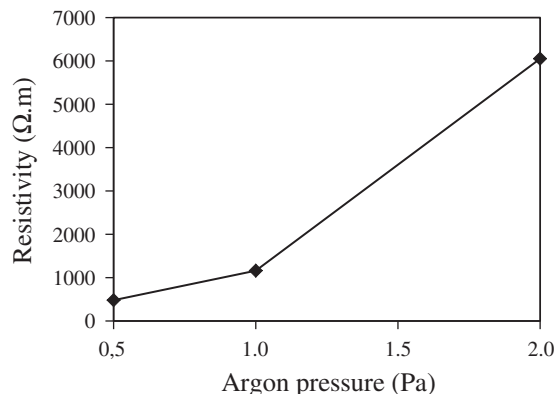


**Fig. 6.** Evolution of electrical resistivity of films measured at 70 °C versus deposition pressure.

control process. Original properties could emerge from these metastable nanostructured materials.

#### References

- [1] K.E. Sickafus, J.M. Wills, N.W. Grimes, Structure of spinel, *J. Am. Ceram. Soc.* 82 (1999) 3279.
- [2] A. Navrotsky, O.J. Kleppa, The thermodynamics of cation distributions in simple spinels, *J. Inorg. Nucl. Chem.* 29 (1967) 2701.
- [3] G.A. Sawatzky, F. Van der Woude, Mössbauer study of several ferrimagnetic spinels, *Phys. Rev.* 187 (1969) 747.
- [4] E.J.W. Verwey, E.L. Heilmann, Physical properties and cation arrangement of oxides with spinel structures – I. Cation arrangement in spinels, *J. Chem. Phys.* 15 (1947) 174.
- [5] A. Miller, Distribution of cations in spinels, *J. Appl. Phys.* 30 (2009) 24.
- [6] E.J. Verwey, P.W. Haayman, F.C. Romeijn, Physical properties and cation arrangement of oxides with spinel structures II. Electronic conductivity, *J. Chem. Phys.* 15 (1947) 181.
- [7] M.R. De Guire, R.C. OHandley, G. Kalonji, The cooling rate dependence of cation distributions in  $\text{CoFe}_2\text{O}_4$ , *J. Appl. Phys.* 65 (1989) 3167.
- [8] P. Umadevi, C.L. Nagendra, Preparation and characterisation of transition metal oxide micro-thermistors and their application to immersed thermistor bolometer infrared detectors, *Sensors Actuators A* 96 (2002) 114.
- [9] Y. Chen, J.E. Snyder, C.R. Schwichtenberg, K.W. Dennis, R.W. Mc-Callum, D.C. Jiles, Metal-bonded Co-ferrite composites for magnetostrictive torque sensor applications, *IEEE Trans. Magn.* 35 (1999) 3652.
- [10] B. Raveau, Strongly correlated electron systems: from chemistry to physics, *C. R. Chim.* 14 (2011) 856.
- [11] S. Walia, S. Balendhran, H. Nili, S. Zhuiykov, G. Rosengarten, Q.H. Wang, M. Bhaskaran, S. Sriram, M.S. Strano, K. Kalantar-Zadeh, Transition metal oxides – thermoelectric properties, *Prog. Mater. Sci.* 58 (2013) 1443.
- [12] S. Roy, S.B. Majumder, Recent advances in multiferroic thin films and composites, *J. Alloys Compd.* 538 (2012) 153.
- [13] S. Basu, K.R. Babu, R.N.P. Choudhary, Studies on the piezoelectric and magnetostrictive phase distribution in lead zirconate titanate-cobalt iron oxide composites, *Mater. Chem. Phys.* 132 (2012) 570.
- [14] H.F. Wang, R. Kavanagh, Y.L. Guo, Y. Guo, G. Lu, P. Hu, Origin of extraordinarily high catalytic activity of  $\text{Co}_3\text{O}_4$  and its morphological chemistry for CO oxidation at low temperature, *J. Catal.* 296 (2012) 110.
- [15] Y. Tan, C. Wu, H. Lin, J. Li, B. Chi, J. Pu, L. Jian, Insight the effect of surface Co cations on the electrocatalytic oxygen evolution properties of cobaltite spinels, *Electrochim. Acta* 121 (2014) 183.
- [16] J. Robin, Recherches sur la constitution et la stabilité de quelques solutions solides à base d'oxyde de cobalt, *Ann. Chim.* 12 (1955) 389.
- [17] J. Robin, J. Benard, Recherches sur la structure et la stabilité des phases dans le système  $\text{Fe}_2\text{O}_3\text{-Co}_3\text{O}_4$ , *C. R. Acad. Sci.* 234 (1952) 734.
- [18] M. Takahashi, M.E. Fine, Coercive force of spinodally decomposed cobalt ferrite with excess cobalt, *J. Am. Ceram. Soc.* 53 (1970) 633.
- [19] M. Takahashi, J.R.C. Guimaraes, M.E. Fine, Spinodal decomposition in the system  $\text{CoFe}_2\text{O}_4\text{-Co}_3\text{O}_4$ , *J. Am. Ceram. Soc.* 54 (1971) 291.
- [20] J.W. Cahn, J.E. Hilliard, Free energy of a nonuniform system. I. Interfacial free energy, *J. Chem. Phys.* 28 (1958) 258.
- [21] S. Hirano, T. Yogo, K. Kikuta, E. Asai, K. Sugiyama, H. Yamamoto, Preparation and phase separation behavior of (Co, Fe)3O4 films, *J. Am. Ceram. Soc.* 76 (1993) 1788.
- [22] K.J. Kim, J.H. Lee, C.S. Kim, Phase decomposition and related structural magnetic properties of iron cobaltite thin films, *J. Korean Phys. Soc.* 61 (2012) 1274.
- [23] H. Le Trong, A. Barnabe, L. Presmanes, P. Tailhades, Phase decomposition study in  $\text{Co}_x\text{Fe}_{3-x}\text{O}_4$  iron cobaltites: synthesis and structural characterization of the spinodal transformation, *Solid State Sci.* 10 (2008) 550.
- [24] H. Le Trong, L. Presmanes, E. De Grave, A. Barnabé, C. Bonningue, Ph. Tailhades, Mössbauer characterisations and magnetic properties of iron cobaltites  $\text{Co}_x\text{Fe}_{3-x}\text{O}_4$

- 4 ( $1 \leq x \leq 2.46$ ) before and after spinodal decomposition, *J. Magn. Magn. Mater.* 334 (2013) 66.
- [25] M.G.M. Miranda, E. Estevez-Rams, G. Martinez, M.N. Baibich, Phase separation in  $\text{Cu}_{90}\text{Co}_{10}$  high-magneto-resistance materials, *Phys. Rev. B* 68 (2003) (article #014434).
- [26] A. Hutten, D. Sudfeld, K. Wojcyrkowski, P. Jutzi, G. Reiss, Giant magneto-resistance and magnetic aspects in granular structures, *J. Magn. Magn. Mater.* 262 (2003) 23.
- [27] S.A. Nikitov, P. Tailhades, C.S. Tsai, Spin waves in periodic magnetic structures-magnonic crystals, *J. Magn. Magn. Mater.* 236 (2001) 320.
- [28] Y.V. Gulyaev, S.A. Nikitov, L.V. Zhiotovskii, A.A. Klimov, P. Tailhades, L. Presmanes, C. Bonningue, C.S. Tsai, S.L. Vysotskii, Y.A. Filimonov, Ferromagnetic films with magnon bandgap periodic structures: magnon crystals, *JETP Lett.* 77 (2003) 567.
- [29] B. Mauvernay, L. Presmanes, C. Bonningue, P. Tailhades, Nanocomposite  $\text{Fe}_{1-x}\text{O}/\text{Fe}_3\text{O}_4$ ,  $\text{Fe}/\text{Fe}_{1-x}$  thin films prepared by RF sputtering and revealed by magnetic coupling effects, *J. Magn. Magn. Mater.* 320 (2008) 58.
- [30] M. Ohring, *Materials Science of Thin Films*, Academic Press, 2001.
- [31] A. Richardt, A.M. Durand, *Les interactions ions énergétiques-solides*, Ed. In Fine, 1997.
- [32] G. Panzner, B. Egert, H.P. Schmidt, The stability of  $\text{CuO}$  and  $\text{Cu}_2\text{O}$  surfaces during argon sputtering studied by XPS and AES, *Surf. Sci.* 151 (1985) 400.
- [33] T.M.A. Bui, H. Le Trong, L. Presmanes, A. Barnabé, C. Bonningue, Ph. Tailhades, Thin films of  $\text{Co}_{1.7}\text{Fe}_{1.3}\text{O}_4$  prepared by radio frequency sputtering – the first step towards their spinodal decomposition, *CrystEngComm* 16 (2014) 3359.
- [34] W.B. White, B.A. De Angelis, Interpretation of the vibrational spectra of spinels, *Spectrochim. Acta A: Mol. Spectrosc.* 23 (1967) 985.
- [35] H. Shirai, Y. Morioka, I. Nakagawa, Infrared and Raman spectra and lattice vibrations of some oxide spinels, *J. Phys. Soc. Jpn.* 51 (1982) 592.
- [36] N. Bahlawane, P.H.T. Ngamou, V. Vannier, T. Kottke, J. Heberle, K. Kohse-Höinghaus, Tailoring the properties and the reactivity of the spinel cobalt oxide, *Phys. Chem. Chem. Phys.* 11 (2009) 9224.
- [37] S. Ayyappan, J. Philip, B. Raj, Effect of digestion time on size and magnetic properties of spinel  $\text{CoFe}_2\text{O}_4$  nanoparticles, *J. Phys. Chem. C* 113 (2009) 590.
- [38] P. Chandramohan, M.P. Srinivasan, S. Velmurugan, S.V. Narasimhan, Cation distribution and particle size effect on Raman spectrum of  $\text{CoFe}_2\text{O}_4$ , *J. Solid State Chem.* 184 (2011) 89.
- [39] G. Shemer, E. Tirosh, T. Livneh, G. Markovich, Tuning a colloidal synthesis to control  $\text{Co}^{2+}$  doping in ferrite nanocrystals, *J. Phys. Chem. C* 111 (2007) 14334.
- [40] T. Yu, Z.X. Shen, Y. Shi, J. Ding, Cation migration and magnetic ordering in spinel  $\text{CoFe}_2\text{O}_4$  powder: micro-Raman scattering study, *J. Phys. Condens. Matter* 14 (2002) L613.
- [41] M. Hanesch, Raman spectroscopy of iron oxides and (oxy)hydroxides at low laser power and possible applications in environmental magnetic studies, *Geophys. J. Int.* 177 (2009) 941.
- [42] F. Oudrhiri-Hassani, L. Presmanes, A. Barnabé, Ph. Tailhades, Microstructure, porosity and roughness of RF sputtered oxide thin films: characterization and modelization, *Appl. Surf. Sci.* 254 (2008) 5796.
- [43] S. Capdeville, P. Alphonse, C. Bonningue, L. Presmanes, Ph. Tailhades, Microstructure and electrical properties of sputter-deposited  $\text{Zn}_{0.87}\text{Fe}_{2.13}\text{O}_4$  thin layers, *J. Appl. Phys.* 96 (2004) 6142.
- [44] N. Viart, R.S. Hassan, J.L. Loison, G. Versini, F. Huber, P. Panissod, C. Mény, G. Pourroy, Exchange coupling in  $\text{CoFe}_2\text{O}_4/\text{CoFe}_2$  bilayers elaborated by pulsed laser deposition, *J. Magn. Magn. Mater.* 279 (2004) 21.
- [45] A. Lisfi, C.M. Williams, L.T. Nguyen, J.C. Lodder, A. Coleman, H. Corcoran, A. Johnson, P. Chang, A. Kumar, W. Morgan, Reorientation of magnetic anisotropy in epitaxial cobalt ferrite thin films, *Phys. Rev. B* 76 (2007) 054405.
- [46] Y. Suzuki, G. Hu, R.B. van Dover, R.J. Cava, Magnetic anisotropy of epitaxial cobalt ferrite thin films, *J. Magn. Magn. Mater.* 191 (1999) 1.
- [47] L. Néel, Aimantation à saturation de certains ferrites, *C. R. Hebd. Séanc. Acad. Sci. Paris* 230 (1950) 190.
- [48] W.H. Meiklejohn, C.P. Bean, New magnetic anisotropy, *Phys. Rev.* 102 (1956) 1413.
- [49] W.H. Meiklejohn, Exchange anisotropy in the iron-iron oxide system, *J. Appl. Phys.* 29 (1958) 454.
- [50] J. Nogués, I.K. Schuller, Exchange bias, *J. Magn. Magn. Mater.* 192 (1999) 203.
- [51] G.H. Jonker, Analysis of the semiconducting properties of cobalt ferrite, *J. Phys. Chem. Solids* 9 (1959) 165.
- [52] G.H. Jonker, S. van Houten, *Semiconducting Properties of Transition Metal Oxides*, Springer, 1959, ISBN 9783540753070.
- [53] P.A. Cox, *Electronic Structure and Chemical of Solids*, Oxford University Press, 1987, ISBN 9780198552048.